

# Supersymmetric Dark Matter Candidates

John Ellis <sup>a</sup> and Keith A. Olive <sup>b</sup>

<sup>a</sup>*TH Division, Physics Department, CERN, Geneva, Switzerland*

<sup>b</sup>*William I. Fine Theoretical Physics Institute, University of Minnesota,  
Minneapolis, MN 55455, USA*

## Abstract

After reviewing the theoretical, phenomenological and experimental motivations for supersymmetric extensions of the Standard Model, we recall that supersymmetric relics from the Big Bang are expected in models that conserve  $R$  parity. We then discuss possible supersymmetric dark matter candidates, focusing on the lightest neutralino and the gravitino. In the latter case, the next-to-lightest supersymmetric particle is expected to be long-lived, and possible candidates include spartners of the tau lepton, top quark and neutrino. We then discuss the roles of the renormalization-group equations and electroweak symmetry breaking in delimiting the supersymmetric parameter space. We discuss in particular the constrained minimal extension of the Standard Model (CMSSM), in which the supersymmetry-breaking parameters are assumed to be universal at the grand unification scale, presenting predictions from a frequentist analysis of its parameter space. We also discuss astrophysical and cosmological constraints on gravitino dark matter models, as well as the parameter space of minimal supergravity (mSUGRA) models in which there are extra relations between the trilinear and bilinear supersymmetry-breaking parameters, and between the gravitino and scalar masses. Finally, we discuss models with non-universal supersymmetry-breaking contributions to Higgs masses, and models in which the supersymmetry-breaking parameters are universal at some scale below that of grand unification.

*From ‘Particle Dark Matter: Observations, Models and Searches’ edited by  
Gianfranco Bertone Copyright 2010 Cambridge University Press. Chapter 8, pp.  
142-163 Hardback ISBN 9780521763684,  
<http://cambridge.org/us/catalogue/catalogue.asp?isbn=9780521763684>*

# 1 Motivations

Supersymmetry is one of the best-motivated proposals for physics beyond the Standard Model. There are many idealistic motivations for believing in supersymmetry, such as its intrinsic elegance, its ability to link matter particles and force carriers, its ability to link gravity to the other fundamental interactions, its essential role in string theory, etc. However, none of these aesthetic motivations gives any hint as to the energy scale at which supersymmetry might appear. The following are the principal utilitarian reasons to think that supersymmetry might appear at some energy accessible to forthcoming experiments.

The first and primary of these was the observation that supersymmetry could help stabilize the mass scale of electroweak symmetry breaking, by cancelling the quadratic divergences in the radiative corrections to the mass-squared of the Higgs boson [1, 2, 3], and by extension to the masses of other Standard Model particles. This motivation suggests that sparticles weigh less than about 1 TeV, but the exact mass scale depends on the amount of fine-tuning that one is prepared to tolerate.

Historically, the second motivation for low-scale supersymmetry, and the one that interests us most here, was the observation that the lightest supersymmetric particle (LSP) in models with conserved  $R$  parity, being heavy and naturally neutral and stable, would be an excellent candidate for dark matter [4, 5]. This motivation requires that the lightest supersymmetric particle should weigh less than about 1 TeV, if it had once been in thermal equilibrium in the early Universe. This would have been the case for a neutralino  $\chi$  or a sneutrino  $\tilde{\nu}$  LSP, and the argument can be extended to a gravitino LSP because it may be produced in the decays of heavier, equilibrated sparticles.

The third reason that emerged for thinking that supersymmetry may be accessible to experiment was the observation that including sparticles in the renormalization-group equations (RGEs) for the gauge couplings of the Standard Model would permit them to unify [6, 7, 8, 9, 10], whereas unification

would not occur if only the Standard Model particles were included in the RGEs. However, this argument does not constrain the supersymmetric mass scale very precisely: scales up to about 10 TeV or perhaps more could be compatible with grand unification.

The fourth motivation is the fact that the Higgs boson is (presumably) relatively light, according to the precision electroweak data - an argument reinforced by the negative results (so far) of searches for the Higgs boson at the Fermilab Tevatron collider. It has been known for some 20 years that the lightest supersymmetric Higgs boson should weigh no more than about 140 GeV, at least in simple models [11, 12, 13, 14, 15]. Since the early 1990s, the precision electroweak noose has been tightening, and the best indication now (incorporating the negative results of searches at LEP and the Tevatron) is that the Higgs boson probably weighs less than about 140 GeV [16, 17], in perfect agreement with the supersymmetric prediction.

Fifthly, if the Higgs boson is indeed so light, the present electroweak vacuum would be destabilized by radiative corrections due to the top quark, unless the Standard Model is supplemented by additional scalar particles [18]. This would be automatic in supersymmetry, and one can extend the argument to ‘prove’ that any mechanism to stabilize the electroweak vacuum must look very much like supersymmetry.

There is a sixth argument that is still controversial, namely the anomalous magnetic moment of the muon,  $g_\mu - 2$ . As is well known, the experimental measurement of this quantity [19] disagrees with the Standard Model prediction [20], if this is calculated using low-energy  $e^+e^-$  annihilation data. On the other hand, the discrepancy with the Standard Model is greatly reduced if one uses  $\tau$  decay data to estimate the Standard Model contribution to  $g_\mu - 2$ . Normally, one would prefer to use  $e^+e^-$  data, since they are related more directly to  $g_\mu - 2$ , with no need to worry about isospin violations, etc. Measurements by the BABAR collaboration using the radiative-return method [21] yield a result intermediate between the previous  $e^+e^-$  data and

$\tau$  decay data. Until the discrepancy between these data sets have been ironed out, one should take  $g_\mu - 2$  *cum grano salis*.

## 2 The MSSM and $R$ parity

We refer to [22, 23] for the general structure of supersymmetric theories. We restrict ourselves here to theories with a single supersymmetry charge, called simple or  $N = 1$  supersymmetry, as these are the only ones able to accommodate chiral fermions and hence the violation of parity and charge conjugation. We recall that the basic building blocks of  $N = 1$  supersymmetric models are so-called chiral supermultiplets, each consisting of a Weyl fermion and a complex scalar, and gauge supermultiplets, each consisting of a gauge field and a gaugino fermion. The renormalizable interactions between the chiral supermultiplets are characterized by a superpotential that couples the chiral supermultiplets in bilinear and trilinear combinations that yield masses and Yukawa interactions, and by gauge interactions. In this framework, bosons and fermions must appear in pairs with identical internal quantum numbers. Since the known particles do not pair up in this way, it is necessary to postulate unseen particles to partner those known in the Standard Model.

In order to construct the minimal supersymmetric extension of the Standard Model (MSSM) [24, 25, 26], one starts with the complete set of chiral fermions needed in the Standard Model, and adds a complex scalar superpartner to each Weyl fermion, so that each matter field in the Standard Model is extended to a chiral supermultiplet. These are denoted by  $L^i, Q^i, e^c, d^c$  and  $u^c$ , where  $i, j$  are  $SU(2)_L$  doublet indices and generation indices have been suppressed as were color indices for the quarks. In order to avoid a triangle anomaly, Higgs supermultiplets must appear in pairs with opposite hypercharges, and the minimal possibility is a single pair  $H_1^i, H_2^i$ . One must also add a gaugino for each of the gauge bosons in the Standard Model so as to

complete the gauge supermultiplets. The minimal supersymmetric standard model (MSSM) [27] is defined by this minimal field content and the minimal superpotential necessary to account for the necessary Yukawa couplings and mass terms, namely:

$$W = \epsilon_{ij}(y_e H_1^j L^i e^c + y_d H_1^j Q^i d^c + y_u H_2^i Q^j u^c) + \epsilon_{ij}\mu H_1^i H_2^j. \quad (1)$$

In (1), the Yukawa couplings,  $y$ , are all  $3 \times 3$  matrices in generation space, with no generation indices for the Higgs multiplets. A second reason for requiring two Higgs doublets in the MSSM is that the superpotential must be a holomorphic function of the chiral superfields. This implies that there would be no way to account for all of the Yukawa terms for both up- and down-type quarks, as well as charged leptons, with a single Higgs doublet. The physical Higgs spectrum then contains five states: two charged Higgs bosons  $H^\pm$ , two scalar neutral Higgs bosons  $h, H$ , and a pseudoscalar Higgs boson  $A$ . The final bilinear mixing term in (1) must be included in the superpotential, in order to avoid a massless Higgs state.

The MSSM must be coupled to gravity, which requires the introduction of a graviton supermultiplet containing a spin-3/2 gravitino as well as the spin-2 graviton itself, which may or not be coupled minimally to the MSSM. The consistency of supergravity at the quantum level requires the breaking of supersymmetry to be spontaneous, with the gravitino mass acting as an order parameter [28, 29]. The mechanism whereby supersymmetry is broken is unknown, as is how this feeds into the MSSM. We adopt here a phenomenological approach, parametrizing the results of this mechanism in terms of differing amounts of explicit supersymmetry breaking in the masses and couplings of the unseen supersymmetric partners of Standard Model particles [30, 31, 23].

In order to preserve the hierarchy between the electroweak and GUT or Planck scales, it is necessary that this explicit breaking of supersymmetry be ‘soft’, i.e., in such a way that the theory remains free of quadratic divergences, which is possible with the insertion of weak scale mass terms in the

Lagrangian [32]. The possible forms for such terms are

$$\begin{aligned}\mathcal{L}_{soft} = & -\frac{1}{2}M^a\lambda^a\lambda^a - \frac{1}{2}(m^2)_{\beta}^{\alpha}\phi_{\alpha}\phi^{\beta*} \\ & -\frac{1}{2}(BM)^{\alpha\beta}\phi_{\alpha}\phi_{\beta} - \frac{1}{6}(Ay)^{\alpha\beta\gamma}\phi_{\alpha}\phi_{\beta}\phi_{\gamma} + h.c.\end{aligned}\quad (2)$$

where the  $M^a$  are masses for the gauginos  $\lambda^a$ ,  $m^2$  is a matrix of soft scalar masses-squared that carries two field indices,  $\alpha, \beta$ , for scalars  $\phi_{\alpha}$ ,  $A$  is a trilinear coupling term with three field indices, and  $B$  is a bilinear supersymmetry breaking term associated with a superpotential bilinear mass term such as  $\mu$  in Eq. 1. Masses for the gauge bosons are, as usual, induced by the spontaneous breaking of gauge invariance, and the masses for chiral fermions are induced by the Yukawa superpotential terms when the electroweak gauge symmetry is broken. For a more complete discussion of supersymmetry and the construction of the MSSM see [33, 34, 35, 36].

In defining the MSSM, we have limited the model to contain a minimal field content: the only new fields are those which are *required* by supersymmetry. Consequently, apart from superpartners, only the Higgs sector was enlarged from one doublet to two. Moreover, in writing the superpotential (1), we have also made a minimal choice regarding interactions. We have limited the types of interactions to include only the minimal set required in the Standard Model and its supersymmetric generalization.

However, even with the minimal field content, there are several other superpotential terms that one could envision adding to (1) which are consistent with all of the gauge symmetries of the theory. Specifically, one could consider adding any or all of the following terms that violate  $R$ -parity:

$$W_R = \frac{1}{2}\lambda\epsilon_{ij}L^iL^je^c + \lambda'\epsilon_{ij}L^iQ^jd^c + \frac{1}{2}\lambda''u^cd^cd^c + \mu'L^iH_2^i. \quad (3)$$

Each of the terms in (3) has one or more suppressed generation indices. We note that the terms proportional to  $\lambda$ ,  $\lambda'$ , and  $\mu'$  both violate lepton number by one unit, whereas the term proportional to  $\lambda''$  violates baryon number by one unit.

Each of the terms in (3) predicts new particle interactions and can be to some extent constrained by the lack of observed exotic phenomena. In particular, any combination of terms which violate both baryon and lepton number would be unacceptable, unless the product of coefficients was extremely small. For example, consider the possibility that both  $\lambda'$  and  $\lambda''$  were non-zero. This would lead to the following proton decay processes:  $p \rightarrow e^+\pi^0, \mu^+\pi^0, \nu\pi^+, \nu K^+$ , etc. The rate of proton decay due to this process would have no suppression by any superheavy masses, since there is no GUT- or Planck-scale physics involved: this is a purely (supersymmetric) Standard Model interaction involving only the electroweak scale. The (inverse) rate can be easily estimated to be

$$\Gamma_p^{-1} \sim \frac{\tilde{m}^4}{m_p^5} \sim 10^8 \text{GeV}^{-1}, \quad (4)$$

assuming a supersymmetry breaking scale of  $\tilde{m}$  of order 100 GeV. This should be compared with current limits to the proton life-time of  $\gtrsim 10^{63} \text{GeV}^{-1}$ . Clearly the product of  $\lambda'$  and  $\lambda''$  must be very small, if not exactly zero.

It is possible to eliminate the unwanted superpotential terms by imposing a discrete symmetry on the theory called  $R$ -parity [37]. This can be represented as

$$R = (-1)^{3B+L+2s}, \quad (5)$$

where  $B$ ,  $L$ , and  $s$  are the baryon number, lepton number, and spin respectively. It is easy to see that, with the definition (5), all the known Standard Model particles have  $R$ -parity +1. For example, the electron has  $B = 0$ ,  $L = -1$ , and  $s = 1/2$ , and the photon has  $B = L = 0$  and  $s = 1$ , so in both cases  $R = 1$ . Similarly, it is clear that all superpartners of the known Standard model particles have  $R = -1$ , since they must have the same value of  $B$  and  $L$  as their conventional partners, but differ by 1/2 unit of spin. If  $R$ -parity is exactly conserved, then all four superpotential terms in (3) must be absent.

The additive conservation of the quantum numbers  $B$ ,  $L$ , and  $s$  implies that  $R$ -parity must be conserved multiplicatively. A first important corollary is that the collisions of conventional particles must always produce supersymmetric particles in pairs, and a second corollary is that heavier supersymmetric particles can decay only into lighter supersymmetric particles. For our purposes here, an even more important corollary of  $R$ -parity conservation is the prediction that the lightest supersymmetric particle (LSP) must be stable, because it has no legal decay mode. In much the same way that baryon number conservation predicts proton stability,  $R$ -parity predicts that the lightest  $R = -1$  state is stable. This makes supersymmetry an extremely interesting theory from the astrophysical point of view, as the LSP naturally becomes a viable dark matter candidate [4, 5].

### 3 Possible Supersymmetric Dark Matter Candidates

What options are available in the MSSM for the stable LSP? Any electrically-charged LSP would bind to conventional matter, and be detectable as an anomalous heavy nucleus, since the ‘Bohr radius’ for the LSP ‘atom’ would be less than the nuclear radius. Similarly, strongly-interacting LSPs would also form anomalous heavy nuclei. However, experiments searching for such objects [38, 39, 40] have excluded their presence on Earth down to an abundance far lower than the expected abundance for the LSP (see below for more details how this is calculated). Therefore, the stable LSP is presumably electrically-neutral and can have only weak interactions. For this reason, the commonly-expected signature of supersymmetric particle production at colliders is missing energy carried away by undetected LSPs.

This still leaves us with several possible dark matter candidates in the MSSM, specifically the sneutrino with spin zero, the neutralino with spin  $1/2$ , and the gravitino with spin  $3/2$ . However, a sneutrino LSP would



have relatively large coherent interactions with heavy nuclei, and experiments searching directly for the scattering of massive dark matter particles on nuclei exclude a stable sneutrino weighing between a few GeV and several TeV [41]. The possible loophole of a very light sneutrino was excluded by measurements of the invisible  $Z$ -boson decay rate at LEP [42].

The LSP candidate that is considered most often is the lightest neutralino. In the MSSM there are four neutralinos, each of which is a linear combination of the following  $R = -1$  neutral fermions [5]: the neutral wino  $\tilde{W}^3$  (the partner of the third component of the  $SU(2)_L$  triplet of weak gauge bosons); the U(1) bino  $\tilde{B}$ ; and two neutral Higgsinos  $\tilde{H}_1$  and  $\tilde{H}_2$  (the supersymmetric partners of the neutral components of the two Higgs doublets).

The composition of the LSP  $\chi$  can be expressed as a linear combination of these fields:

$$\chi = \alpha \tilde{B} + \beta \tilde{W}^3 + \gamma \tilde{H}_1 + \delta \tilde{H}_2, \quad (6)$$

whose mass and composition are determined by the  $SU(2)_L$  and U(1) gaugino masses,  $M_{2,1}$ , the Higgs mixing parameter  $\mu$ , and  $\tan\beta$ , the ratio of the vacuum expectation values  $v_{1,2} \equiv \langle 0|H_{1,2}|0 \rangle$  of the two neutral Higgs fields  $\tan\beta \equiv v_2/v_1$ . The mass of the LSP  $\chi$  and the mixing coefficients  $\alpha, \beta, \gamma$  and  $\delta$  in (6) for the neutralino components that compose the LSP can be found by diagonalizing the mass matrix

$$(\tilde{W}^3, \tilde{B}, \tilde{H}_1^0, \tilde{H}_2^0) \begin{pmatrix} M_2 & 0 & \frac{-g_2 v_1}{\sqrt{2}} & \frac{g_2 v_2}{\sqrt{2}} \\ 0 & M_1 & \frac{g_1 v_1}{\sqrt{2}} & \frac{-g_1 v_2}{\sqrt{2}} \\ \frac{-g_2 v_1}{\sqrt{2}} & \frac{g_1 v_1}{\sqrt{2}} & 0 & -\mu \\ \frac{g_2 v_2}{\sqrt{2}} & \frac{-g_1 v_2}{\sqrt{2}} & -\mu & 0 \end{pmatrix} \begin{pmatrix} \tilde{W}^3 \\ \tilde{B} \\ \tilde{H}_1^0 \\ \tilde{H}_2^0 \end{pmatrix}, \quad (7)$$

In different regions of the supersymmetric parameter space, the LSP may be more bino-like, wino-like, or Higgsino-like, depending on the relative magnitudes of the coefficients  $\alpha, \beta, \gamma$  and  $\delta$ .

The relic abundance of an LSP candidate such as the lightest neutralino is calculated by solving the Boltzmann equation for the LSP number density

in an expanding Universe:

$$\frac{dn}{dt} = -3\frac{\dot{R}}{R}n - \langle\sigma v\rangle(n^2 - n_0^2), \quad (8)$$

where  $n_0$  is the equilibrium number density of neutralinos. Defining the quantity  $f \equiv n/T^3$ , we can rewrite this equation in terms of the reduced temperature  $x \equiv T/m_\chi$ :

$$\frac{df}{dx} = m_\chi \left( \frac{8\pi^3}{90} G_N N \right)^{-1/2} \langle\sigma v\rangle (f^2 - f_0^2), \quad (9)$$

where  $G_N$  is Newton's constant and  $N$  is the number of relativistic degrees of freedom at a given temperature. The solution to this equation at late times and low temperatures, and hence small  $x$ , yields a constant value of  $f$ , so that  $n \propto T^3$ .

The technique [43] used to determine the neutralino relic density is similar to that used previously for computing the relic abundance of massive neutrinos [44, 45, 46], with the substitution of the appropriate annihilation cross section. This and hence the relic density depend on additional parameters in the MSSM beyond  $M_1, M_2, \mu$ , and  $\tan\beta$ , which include the sfermion masses,  $m_{\tilde{f}}$  and mass of the pseudoscalar Higgs boson,  $m_A$ . In much of the parameter space of interest, the LSP is a bino and the annihilation proceeds mainly through crossed  $t$ -channel sfermion exchange. The exception is if the sum of two neutralino masses happens to lie near a direct-channel pole, such as  $m_\chi \simeq m_Z/2$  or  $m_h/2$ , in which case there are large contributions to the annihilation through direct  $s$ -channel resonance exchange. Since the neutralino is a Majorana fermion, away from such a resonance the  $s$ -wave part of the annihilation cross section is generally suppressed by the outgoing fermion masses, and the annihilation occurs mainly through the  $p$  wave, which is also suppressed because the annihilating LSPs are non-relativistic at low temperatures (small  $x$ ). This means that one can approximate the annihilation cross section including  $p$ -wave corrections by incorporating a term proportional to

the temperature if neutralinos are in thermal equilibrium:  $\sigma v = a + bx + \dots$ , where the expansion coefficients  $a, b$  are model-dependent.

Annihilations in the early Universe continue until the annihilation rate  $\Gamma \simeq \sigma v n_\chi$  drops below the expansion rate, after which it is a good first approximation to assume that annihilations are negligible - the freeze-out approximation. The final neutralino relic density, expressed as a fraction  $\Omega_\chi$  of the critical energy density and denoting the present-day Hubble expansion rate as  $h$  in units of 100 km/s/Mpc, can be written as [5]

$$\Omega_\chi h^2 \simeq 1.9 \times 10^{-11} \left( \frac{T_\chi}{T_\gamma} \right)^3 N_f^{1/2} \left( \frac{\text{GeV}}{ax_f + \frac{1}{2}bx_f^2} \right), \quad (10)$$

where  $(T_\chi/T_\gamma)^3$  accounts for the subsequent reheating of the photon temperature with respect to  $\chi$ , due to the annihilations of particles with mass  $m < x_f m_\chi$  [47, 48], and  $x_f = T_f/m_\chi$  is proportional to the freeze-out temperature  $T_f$ . Eq. (10) yields a very good approximation to the relic density except near direct  $s$ -channel annihilation poles or thresholds, and in regions where the LSP is nearly degenerate with the next lightest supersymmetric particle [49].

When there are several particle species  $i$  that are nearly degenerate in mass, coannihilations between the different species become important. In this case [49], the rate equation (8) still applies, provided  $n$  is interpreted as the total number density,

$$n \equiv \sum_i n_i, \quad (11)$$

$n_0$  is interpreted as the total equilibrium number density,

$$n_0 \equiv \sum_i n_{0,i}, \quad (12)$$

and the effective annihilation cross section as

$$\langle \sigma_{\text{eff}} v_{\text{rel}} \rangle \equiv \sum_{ij} \frac{n_{0,i} n_{0,j}}{n_0^2} \langle \sigma_{ij} v_{\text{rel}} \rangle. \quad (13)$$

In eq. (9),  $m_\chi$  is now understood to be the mass of the lightest sparticle under consideration.

We turn finally to the third LSP candidate within the MSSM, namely the gravitino. Since it has only gravitational-strength interactions, it is not expected to have been in thermal equilibrium in the early Universe. However, it could have been produced in high-energy particle collisions in the early Universe, or in the decays of heavier supersymmetric particles. The fact that the gravitino has only gravitational-strength interactions implies that only decays of the next-to-lightest supersymmetric particle (NLSP) would be significant sources of gravitinos, and the NLSP would be metastable. As we discuss in more detail later, there are important cosmological and astrophysical constraints on the possible mass and lifetime of the NLSP, derived principally from the agreement between astrophysical observations and Big-Bang Nucleosynthesis calculations of light-element abundances.

What might be the nature of the NLSP be in such a gravitino LSP scenario? One option is the lighter of the two supersymmetric partners of the  $\tau$  lepton, denoted by  $\tilde{\tau}_1$ . Being a metastable charged particle, it would have a distinctive experimental signature at the LHC or other colliders. Studies within such a scenario have shown that the mass of the  $\tilde{\tau}_1$  could be measured very accurately, and that one could easily reconstruct heavier sparticles that decay into the  $\tilde{\tau}_1$  [50].

Alternatively, the NLSP might be the lighter supersymmetric partner of the top quark, denoted by  $\tilde{t}_1$  [51, 52, 53], which would have even more distinctive signatures at the LHC. Immediately after production, it would become confined inside a charged or neutral hadron. As it moves through an LHC detector, it would have a high probability of changing its charge as it interacts with the material in the detector. This combined with its non-relativistic velocity would provide a truly distinctive signature.

Yet another possibility is that the NLSP might be some flavour of sneutrino [54], in which case the characteristic signature would be missing energy

carried away by the metastable sneutrino. This could nevertheless be distinguished from the conventional missing-energy signature of a neutralino LSP (or NLSP), because the final states would be more likely to include the charged lepton with the same flavour as the sneutrino NLSP, either  $e$ ,  $\mu$  or  $\tau$ .

These are just a few examples of the possible alternatives to the conventional missing-energy signature of supersymmetry. Studies have shown that the LHC would also have good prospects for detecting such signatures.

## 4 Renormalization-Group Equations and Electroweak Symmetry Breaking

The fact that measurements of the strengths of the Standard Model gauge interactions measured at low energies are in excellent agreement with the predictions of a supersymmetric gauge theory [6, 7, 8, 9, 10] was already cited as an important motivation for low-energy supersymmetry. It can also be regarded as a motivation for thinking that other parameters of the effective low-energy theory, e.g., the soft supersymmetry breaking parameters can also be calculated and related using renormalization-group equations (RGEs) below the grand unification scale. For example, the one-loop RGEs for the gaugino masses are:

$$\frac{dM_i}{dt} = -b_i \alpha_i M_i / 4\pi \quad (14)$$

If the gaugino masses have a common value  $m_{1/2}$  at the grand unification scale, these equations can be used to relate the physical low-energy, on-shell values of the gaugino masses to the corresponding gauge coupling strengths  $\alpha_i$ :

$$M_i(t) = \frac{\alpha_i(t)}{\alpha_i(M_{GUT})} m_{1/2}, \quad (15)$$

which implies that

$$\frac{M_1}{g_1^2} = \frac{M_2}{g_2^2} = \frac{M_3}{g_3^2} \quad (16)$$

at the one-loop level. When applying this relation within a specific grand unified theory, one must remember to incorporate the difference of the normalization of the U(1) factor from that in the Standard Model, so that we have  $M_1 = \frac{5}{3} \frac{\alpha_1}{\alpha_2} M_2$  for the one-loop relation between the bino and wino masses. Also, the simple relations (16) are modified by threshold corrections at the electroweak scale, and by two-loop effects in the RGEs. The soft supersymmetry-breaking scalar masses-squared  $m^2$  and the trilinear couplings  $A$  are renormalized analogously to (14), with the difference that Yukawa interactions contribute as well as gauge interactions. However, the Yukawa contributions are small, except for the supersymmetric partners of third-generation fermions.

As described above, the MSSM has over 100 undetermined parameters, which are mainly associated with the breaking of supersymmetry. It is often assumed that the soft supersymmetry-breaking parameters  $M^a, m^2$  and  $A$  have some universality properties. There are phenomenological arguments, based on the success of the Standard Model in describing the observed suppression of flavour-changing interactions, that, at some input scale (often assumed to be that of grand unification), the parameters  $m^2$  and  $A$  must be universal for supersymmetric particles with the same gauge quantum numbers, e.g., the supersymmetric partners of the  $e, \mu$  and  $\tau$ . There is no strong argument why these parameters should be universal for supersymmetric particles with different quantum numbers, e.g.,  $d, u$  and  $e$ , though this may occur in some grand unified theories, as may unification of the gaugino masses  $M^a$ . The simplified version of the MSSM in which universality at the grand unification scale is assumed for each of  $M^a, m^2$  and  $A$  is called the constrained MSSM (CMSSM)[55, 56, 57, 58, 59, 60, 61, 62, 63, 64, 65, 66, 67, 68, 69, 70, 71, 72, 73, 74, 75, 76, 77, 78].

Once one has chosen a set of boundary conditions at the grand unification scale and run the RGEs down to the electroweak scale, one must check the properties of the electroweak vacuum, which are characterized by speci-

fying the mass of the  $Z$  boson,  $M_Z$ , and the ratio of the two Higgs vacuum expectation values,  $\tan\beta$ . These electroweak symmetry-breaking conditions should be used as consistency conditions on the solutions to the RGEs, e.g., of the CMSSM. They are frequently used to fix, as functions of the input values of the common gaugino mass  $m_{1/2}$ ,  $m$ ,  $A$  and  $\tan\beta$ , the magnitudes of the Higgs mixing mass parameter,  $\mu$ , and of the bilinear coupling,  $B$ , which determines the pseudoscalar Higgs mass,  $m_A$ . The sign of  $\mu$  remains free.

An example of the running of the mass parameters in the CMSSM as functions of the renormalization scale is shown in Fig. 1, using as inputs the choices  $m_{1/2} = 250$  GeV,  $m_0 = 100$  GeV,  $\tan\beta = 3$ ,  $A_0 = 0$ , and  $\mu < 0$ . We notice in the figure several characteristic features of the sparticle spectrum. For example, the colored sparticles are typically the heaviest, because of the large positive corrections to their masses arising from  $\alpha_3$ -dependent terms in the RGEs. Also, one finds that the bino,  $\tilde{B}$ , is typically the lightest sparticle. Most importantly, we notice that one of the Higgs masses squared, goes negative, triggering electroweak symmetry breaking [79, 80, 81, 82, 83]. (The negative sign in the figure refers to the sign of the mass squared, even though it is the mass of the sparticles which is depicted.)

## 5 The CMSSM

For given values of  $\tan\beta$ ,  $A_0$ , and  $\text{sgn}(\mu)$ , the regions of the CMSSM parameter space that yield an acceptable relic density and satisfy the other phenomenological constraints may conveniently be displayed in the  $(m_{1/2}, m_0)$  plane. Fig. 2 displays, for  $\tan\beta = 10$  (a) and 50 (b), the impacts of the most relevant constraints. These include the LEP lower limits on the chargino mass:  $m_{\chi^\pm} > 104$  GeV [84], on the selectron mass:  $m_{\tilde{e}} > 99$  GeV [85] and on the Higgs mass:  $m_h > 114$  GeV [86, 87]. The former two constrain  $m_{1/2}$  and  $m_0$  directly via the sparticle masses, and the latter indirectly via the sensitivity of radiative corrections to the Higgs mass to the sparticle masses,

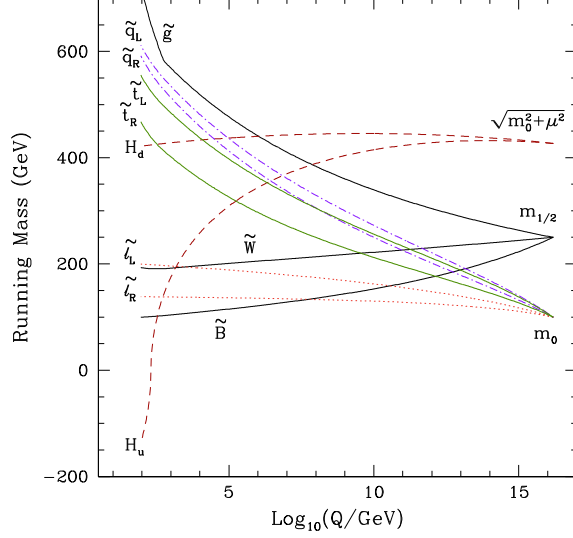


Figure 1: *The renormalization-group evolution of the mass parameters in the CMSSM, assuming  $m_{1/2} = 250$  GeV,  $m_0 = 100$  GeV,  $\tan\beta = 3$ ,  $A_0 = 0$ , and  $\mu < 0$ . We thank Toby Falk for providing this figure.*

principally  $m_{\tilde{t}_1\tilde{b}_1}$ . Here the code FeynHiggs [88, 89] is used for the calculation of  $m_h$ . It would be prudent to assign an uncertainty of 3 GeV to this calculation. Nevertheless, the Higgs limit imposes important constraints, principally on  $m_{1/2}$  and particularly at low  $\tan\beta$ . Another constraint is the requirement that the branching ratio for  $b \rightarrow s\gamma$  be consistent with the experimental measurements [90]. These measurements agree with the Standard Model, and therefore provide bounds on MSSM particles [91], such as the chargino and charged Higgs bosons, in particular. Typically, the  $b \rightarrow s\gamma$  constraint is more important for  $\mu < 0$ , but it is also relevant for  $\mu > 0$ , particularly when  $\tan\beta$  is large. The constraint imposed by measurements of  $b \rightarrow s\gamma$  also exclude small values of  $m_{1/2}$ . Finally, there are regions of the  $(m_{1/2}, m_0)$  plane that are favoured by the Brookhaven National Laboratory measurement [19]



of  $g_\mu - 2$ . Here we assume the Standard Model calculation [20] of  $g_\mu - 2$  using  $e^+e^-$  data, and indicate by dashed and solid lines the contours of 1- and 2- $\sigma$  level deviations induced by supersymmetry.

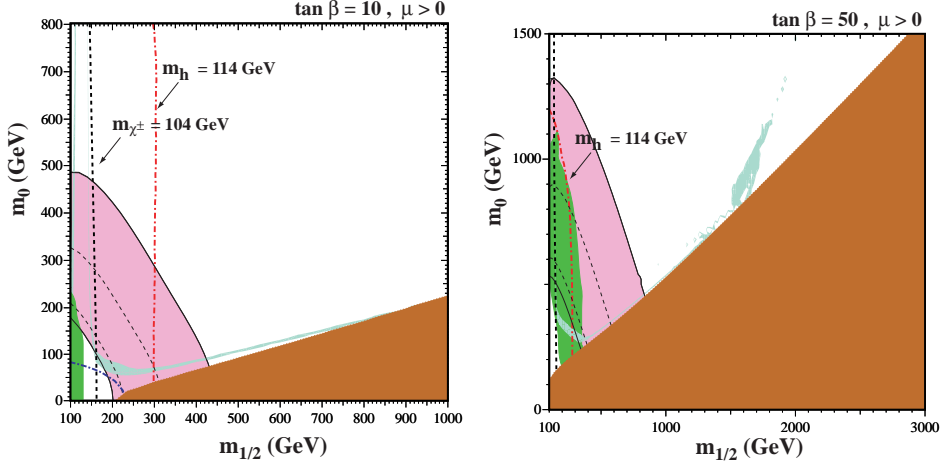


Figure 2: The  $(m_{1/2}, m_0)$  planes for (a)  $\tan\beta = 10$  and (b)  $\tan\beta = 50$ , assuming  $\mu > 0$ ,  $A_0 = 0$ ,  $m_t = 175$  GeV and  $m_b(m_b)_{SM}^{\overline{MS}} = 4.25$  GeV. The near-vertical (red) dot-dashed lines are the contours for  $m_h = 114$  GeV, and the near-vertical (black) dashed line is the contour  $m_{\chi^\pm} = 104$  GeV. Also shown by the dot-dashed curve in the lower left is the region excluded by the LEP bound  $m_{\tilde{e}} > 99$  GeV. The medium (dark green) shaded region is excluded by  $b \rightarrow s\gamma$ , and the light (turquoise) shaded area is the cosmologically preferred region. In the dark (brick red) shaded region, the LSP is the charged  $\tilde{\tau}_1$ . The region allowed by the E821 measurement of  $a_\mu$  at the 2- $\sigma$  level, is shaded (pink) and bounded by solid black lines, with dashed lines indicating the 1- $\sigma$  ranges.

The most precise constraint on supersymmetry may be that provided by the density of cold dark matter, as determined from astrophysical and cosmological measurements by WMAP and other experiments [92]:

$$\Omega_{CDM} = 0.1099 \pm 0.0062. \quad (17)$$

Applied straightforwardly to the relic LSP density  $\Omega_{LSP} h^2$ , this would give a very tight relation between supersymmetric model parameters, fixing some

combination of them at the % level, which would essentially reduce the dimensionality of the supersymmetric parameter space by one unit. Let us assume for now that the LSP is the lightest neutralino  $\chi$ , whose density is usually thought to be fixed by freeze-out from thermal equilibrium in the early Universe, as discussed previously. In this case, respecting the constraint (17) would force the CMSSM into one of the narrow WMAP ‘strips’ in planar projections of the parameters [74], as illustrated by the narrow light (turquoise) regions in Fig. 2. However, caution should be exercised before jumping to this conclusion.

Supersymmetry might not be the only contribution to the cold dark matter, in which case (17) should be interpreted as an upper limit on  $\Omega_{LSP} h^2$ . However, most of the supersymmetric parameter space in simple models gives a supersymmetric relic density that exceeds the WMAP range (17), e.g., above the WMAP ‘strip’ in Fig. 2, and the regions with lower density generally correspond to *lower* values of the sparticle masses, i.e., below the WMAP ‘strip’ in Fig. 2.

However, even if one takes them seriously, the locations of these WMAP ‘strips’ do vary significantly with the choices of other supersymmetric parameters, as can be seen by comparing the cases of  $\tan \beta = 10, 50$  in Fig. 2(a, b). As one varies  $\tan \beta$ , the WMAP ‘strips’ cover much of the  $(m_{1/2}, m_0)$  plane.

Several different regions of the WMAP ‘strips’ in the CMSSM  $(m_{1/2}, m_0)$  plane can be distinguished, in which different dynamical processes are dominant. At low values of  $m_{1/2}$  and  $m_0$ , simple  $\chi - \chi$  annihilations via crossed-channel sfermion exchange are dominant, but this ‘bulk’ region is now largely excluded by the LEP lower limit on the Higgs mass,  $m_h$ . At larger  $m_{1/2}$ , but relatively small  $m_0$ , close to the boundary of the region where the lighter stau is lighter than the lightest neutralino:  $m_{\tilde{\tau}_1} < m_\chi$ , coannihilation between the  $\chi$  and sleptons are important in suppressing the relic  $\chi$  density into the WMAP range (17), as seen in Fig. 2. At larger  $m_{1/2}, m_0$  and  $\tan \beta$ , the relic  $\chi$  density may be reduced by rapid annihilation through direct-

channel  $H, A$  Higgs bosons, as seen in Fig. 2(b). Finally, the relic density can again be brought down into the WMAP range (17) at large  $m_0$  (not shown in Fig. 2), in the ‘focus-point’ region close the boundary where electroweak symmetry breaking ceases to be possible and the lightest neutralino  $\chi$  acquires a significant higgsino component [93].

As seen in Fig. 2, the relic density constraint is compatible with relatively large values of  $m_{1/2}$  and  $m_0$ , and it is interesting to look for any indication where the supersymmetric mass scale might lie within this range, using the available phenomenological and cosmological constraints. A global likelihood analysis enables one to pin down the available parameter space in the CMSSM and the related models discussed later. One can avoid the dependence on priors by performing a pure likelihood analysis as in [94], or a purely  $\chi^2$ -based fit as done in [95, 96]. Here we present results from one such analysis [97], which used a Markov-Chain Monte Carlo (MCMC) technique to explore efficiently the likelihood function in the parameter space of the CMSSM. A full list of the observables and the values assumed for them in this global analysis are given in [96], as updated in [97].

The 68% and 95% confidence-level (C.L.) regions in the  $(m_{1/2}, m_0)$  plane of the CMSSM are shown in Fig. 3 [97]. Also shown for comparison are the physics reaches of ATLAS and CMS with 1/fb of integrated luminosity [98, 99]. (MET stands for missing transverse energy, SS stands for same-sign dilepton pairs, and the sensitivity for finding the lightest Higgs boson in cascade decays of supersymmetric particles is calculated for 2/fb of data.) The likelihood analysis assumed  $\mu > 0$ , as motivated by the sign of the apparent discrepancy in  $g_\mu - 2$ , but sampled all values of  $\tan\beta$  and  $A_0$ : the experimental sensitivities were estimated assuming  $\tan\beta = 10$  and  $A_0 = 0$ , but are probably not very sensitive to these assumptions. The global maxima of the likelihood function (indicated by the black dot) is at  $m_{1/2} = 310$  GeV,  $m_0 = 60$  GeV,  $A_0 = 240$  GeV,  $\tan\beta = 11$  and  $\chi^2/N_{dof} = 20.4/19$  (37% probability). It is encouraging that the best-fit points lie well within the LHC

discovery range, as do the 68% and most of the 95% C.L. regions. It is also encouraging that the two best-fit points have similar values of  $m_{1/2}$ ,  $m_0$  and  $\tan\beta$ , the most important parameters for the sparticle spectrum, indicating that the likelihood analysis is relatively insensitive to the theoretical model assumptions.

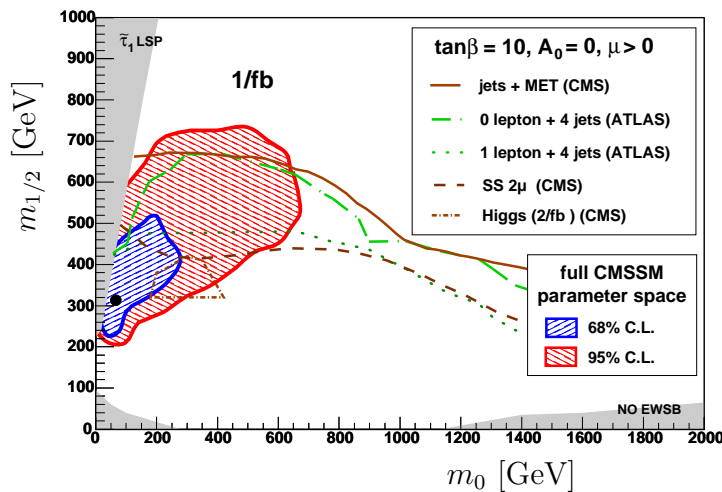


Figure 3: The  $(m_0, m_{1/2})$  plane in the CMSSM showing the regions favoured in a likelihood analysis at the 68% (blue) and 95% (red) confidence levels [97]. The best-fit point is shown as the black point. Also shown are the discovery contours in different channels for the LHC with 1/fb (2/fb for the Higgs search in cascade decays of sparticles) [98, 99].

In contrast to this neutralino LSP scenario, the gravitino dark matter (GDM) scenario in the CMSSM is tightly constrained by the astrophysical constraints on the cosmological abundances of light elements, as seen in Fig. 4 [100]. However, such a scenario might have some advantages, e.g., by enabling the cosmological prediction for the abundance of  $^7\text{Li}$  [101] to be improved, as also shown in Fig. 4(b).

Recently, new attention has been focussed on the regions in which a metastable stau is the next-to-lightest sparticle (NSP) in a GDM scenario,

due to its ability to form bound states (primarily with  $^4\text{He}$ ). When such bound states occur, they catalyze certain nuclear reactions such as  $^4\text{He}(\text{D}, \gamma)^6\text{Li}$ , which is normally highly suppressed due to the production of a low-energy  $\gamma$ , whereas the bound-state reaction is not [102, 103, 104]. In Fig. 4(a), the  $(m_{1/2}, m_0)$  plane is displayed showing explicit element abundance contours [100] when the gravitino mass is  $m_{3/2} = 0.2m_0$  in the *absence* of stau bound-state effects. To the left of the solid black line the gravitino is not the LSP. The diagonal red dotted line corresponds to the boundary between a neutralino and stau NSP: above it, the neutralino is the NSP, and below it, the stau is the NSP. Very close to this boundary, there is a diagonal brown solid line. Above this line, the relic density of gravitinos from NSP decay is too high, i.e.,

$$\frac{m_{3/2}}{m_{NSP}}\Omega_{NSP}h^2 > 0.12. \quad (18)$$

Thus we should restrict our attention to the area below this line.

The very thick green line labelled  $^7\text{Li} = 4.3$  corresponds to the contour where  $^7\text{Li}/\text{H} = 4.3 \times 10^{-10}$ , a value very close to the standard BBN result for  $^7\text{Li}/\text{H}$ . It forms a ‘Vee’ shape, whose right edge runs along the neutralino-stau NSP border. Below the Vee, the abundance of  $^7\text{Li}$  is smaller than the standard BBN result. However, for relatively small values of  $m_{1/2}$ , the  $^7\text{Li}$  abundance does not differ very much from the standard BBN result: it is only when  $m_{1/2} \gtrsim 3000$  GeV that  $^7\text{Li}$  begins to drop significantly. The stau lifetime drops with increasing  $m_{1/2}$ , and when  $\tau \sim 1000$  s, at  $m_{1/2} \sim 4000$  GeV, the  $^7\text{Li}$  abundance has been reduced to an observation-friendly value close to  $2 \times 10^{-10}$  as reported in [105, 106] and shown by the (unlabeled) thin dashed (green) contours.

The region where the  $^6\text{Li}/^7\text{Li}$  ratio lies between 0.01 and 0.15 forms a band which moves from lower left to upper right. As one can see in the orange shading, there is a large region where the lithium isotopic ratio can be made acceptable. However, if we restrict to  $\text{D}/\text{H} < 4.0 \times 10^{-5}$ , we see that this ratio is interesting only when  $^7\text{Li}$  is at or slightly below the standard

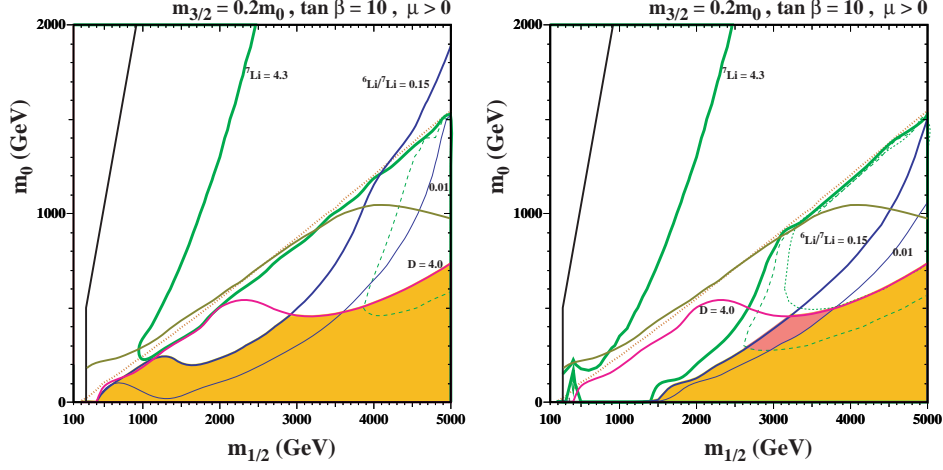


Figure 4: The  $(m_{1/2}, m_0)$  planes for  $m_t = 172.7$  GeV,  $A_0 = 0$ ,  $\mu > 0$  and  $\tan\beta = 10$  with  $m_{3/2} = 0.2m_0$  without (a) and with (b) the effects of metastable stau bound states included. The regions to the left of the solid black lines are not considered, since there the gravitino is not the LSP. In the orange (light) shaded regions, the differences between the calculated and observed light-element abundances are no greater than in standard BBN without late particle decays. In the pink (dark) shaded region in panel (b), the abundances lie within the ranges favoured by observation. The significances of the other lines and contours are explained in the text.

BBN result.

Turning now to Fig. 4(b), we show the analogous results when the bound-state effects are included in the calculation. The abundance contours are identical to those in panel (a) above the diagonal dotted line, where the NSP is a neutralino and bound states do not form. We also note that the bound-state effects on D and  $^3\text{He}$  are quite minimal, so that these element abundances are very similar to those in Fig. 4(a). However, comparing panels (a) and (b), one sees dramatic bound-state effects on the lithium abundances. Everywhere to the left of the solid blue line labeled 0.15 is excluded. In the stau NSP region, this means that  $m_{1/2} \gtrsim 1500$  GeV. Moreover, in the stau region to the right of the  $^6\text{Li}/^7\text{Li} = 0.15$  contour, the  $^7\text{Li}$  abundance

drops below  $9 \times 10^{-11}$  (as shown by the thin green dotted curve). In this case, not only do the bound-state effects increase the  ${}^6\text{Li}$  abundance when  $m_{1/2}$  is small (i.e., at relatively long stau lifetimes), but they also decrease the  ${}^7\text{Li}$  abundance when the lifetime of the stau is about 1500 s. Thus, at  $(m_{1/2}, m_0) \simeq (3200, 400)$  GeV, we find that  ${}^6\text{Li}/{}^7\text{Li} \simeq 0.04$ ,  ${}^7\text{Li}/\text{H} \simeq 1.2 \times 10^{-10}$ , and  $\text{D}/\text{H} \simeq 3.8 \times 10^{-5}$ . Indeed, when  $m_{1/2}$  is between 3000–4000 GeV, the bound-state effects cut the  ${}^7\text{Li}$  abundance roughly in half. In the darker (pink) region, the lithium abundances match the observational plateau values, with the properties  ${}^6\text{Li}/{}^7\text{Li} > 0.01$  and  $0.9 \times 10^{-10} < {}^7\text{Li}/\text{H} < 2.0 \times 10^{-10}$ . This example demonstrates that it is possible to resolve the  ${}^6\text{Li}/{}^7\text{Li}$  by postulating GDM with a stau NSP.

## 6 mSUGRA

Minimal supergravity (mSUGRA) is often used as a basis for phenomenological studies [30, 23, 107]. The framework termed above the CMSSM is occasionally referred to as the mSUGRA. However, models based strictly on minimal supergravity should employ two additional constraints [108, 109]. One is a relation between the soft supersymmetry-breaking bilinear and trilinear parameters:  $B_0 = A_0 - m_0$ , and the other is a relation between the gravitino and input scalar masses:  $m_{3/2} = m_0$ . In the simplest version of mSUGRA [110, 30, 23, 107], where supersymmetry is broken by a single field in a hidden sector, the universal trilinear soft supersymmetry-breaking terms are  $A_0 = (3 - \sqrt{3})m_0$  and bilinear soft supersymmetry-breaking term is  $B_0 = (2 - \sqrt{3})m_0$ , which is a special case of the general relation  $B_0 = A_0 - m_0$ .

Given such a relation between  $B_0$  and  $A_0$ , one can no longer use the standard CMSSM boundary conditions, in which  $m_{1/2}$ ,  $m_0$ ,  $A_0$ ,  $\tan\beta$ , and  $\text{sgn}(\mu)$  are input at the GUT scale, and then  $\mu$  and  $B$  are determined by the electroweak symmetry-breaking conditions. In this case, it is natural to use  $B_0$  as an input and calculate  $\tan\beta$  from the minimization of the Higgs

potential [108, 109].

Phenomenologically distinct planes may be determined by specifying a choice for  $A_0/m_0$ , with the above-mentioned simplest hidden sector being one example. In Fig. 5, two such planes are shown assuming  $m_t = 172.7$  GeV with (a)  $A_0/m_0 = 3 - \sqrt{3}$ , as predicted in the simplest model of supersymmetry breaking [110], and with (b)  $A_0/m_0 = 2.0$ . We show in these  $(m_{1/2}, m_0)$  planes the contours of  $\tan\beta$  as solid blue lines. Also shown are the contours where  $m_{\chi^\pm} > 104$  GeV (near-vertical black dashed lines) and  $m_h > 114$  GeV (diagonal red dash-dotted lines). The regions excluded by  $b \rightarrow s\gamma$  have medium (green) shading, those where the relic density of neutralinos lies within the WMAP range have light (turquoise) shading, and the region suggested by  $g_\mu - 2$  at  $2\text{-}\sigma$  has very light (yellow) shading, as in the CMSSM planes shown previously. As one can see, relatively low values of  $\tan\beta$  are obtained in most of the visible planes.

Another difference between the CMSSM and models based on mSUGRA concerns the mass of the gravitino. In the CMSSM, it is not specified and can be taken suitably large so that the neutralino or the lighter stau is the LSP. In mSUGRA, the scalar masses at the GUT scale,  $m_0$ , are determined by (and equal to) the gravitino mass. In Fig. 5, the gravitino LSP and the neutralino LSP regions are separated by dark (chocolate) solid lines. Above these lines, the neutralino (or stau) is the LSP, whilst below them the gravitino is the LSP [111, 112, 113]. As one can see by comparing the two panels, the potential for neutralino dark matter in mSUGRA models is dependent on  $A_0/m_0$ . In panel (a), the only areas where the neutralino density are not too large occur where the Higgs mass is far too small or, at higher  $m_0$ , the chargino mass is too small. At larger  $A_0/m_0$ , the coannihilation strip rises above the neutralino-gravitino LSP boundary. In panel (b), we see the familiar coannihilation strip. It should be noted that the focus-point region is not realized in mSUGRA models as the value of  $\mu$  does not decrease with increasing  $m_0$  when  $A_0/m_0$  is fixed and  $B_0 = A_0 - m_0$ . There are also no



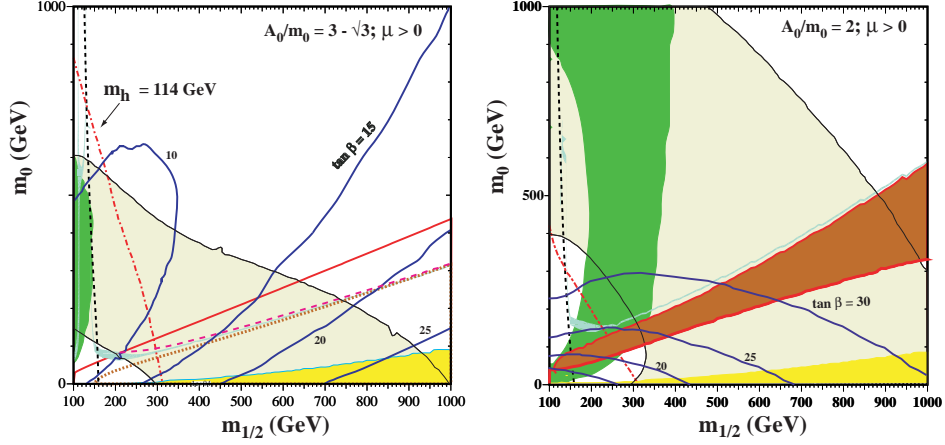


Figure 5: *Examples of  $mSUGRA$   $(m_{1/2}, m_0)$  planes with contours of  $\tan \beta$  superposed, for  $\mu > 0$  and (a) the simplest Polonyi model with  $A_0/m_0 = 3 - \sqrt{3}$ , and (b)  $A_0/m_0 = 2.0$ , all with  $B_0 = A_0 - m_0$ . In each panel, we show the regions excluded by the LEP lower limits on MSSM particles and those ruled out by  $b \rightarrow s\gamma$  decay (medium green shading): the regions favoured by  $g_\mu - 2$  are very light (yellow) shaded, bordered by a thin (black) line. The dark (chocolate) solid lines separate the neutralino and gravitino LSP regions. The regions favoured by WMAP in the neutralino LSP case have light (turquoise) shading. The dashed (pink) line corresponds to the maximum relic density for the gravitino LSP, and regions allowed by BBN constraint neglecting the effects of bound states on NSP decay are light (yellow) shaded.*

funnel regions, as  $\tan \beta$  is never sufficiently high.

In the gravitino LSP regions, the NSP may be either the neutralino or stau, which are now unstable. (Note that in panel (b) there is also a region which is excluded because the stau is the LSP.) The relic density of gravitinos is acceptably low only below the dashed (pink) line. This excludes a supplementary domain of the  $(m_{1/2}, m_0)$  plane in panel (a) which has a neutralino NSP (the dotted (red) curve in panel (a) separates the neutralino and stau NSP regions). However, the strongest constraint is provided by the effect of neutralino or stau decays on Big-Bang Nucleosynthe-

sis [114, 115, 116, 117, 118, 119]. Outside the light (yellow) shaded region, the decays spoil the success of BBN.

## 7 Other Possibilities

These cosmologically preferred regions move around in the  $(m_{1/2}, m_0)$  plane if one abandons the universality assumptions of the CMSSM. For example, if one allows the supersymmetry-breaking contributions to the Higgs masses to be non-universal (NUHM), the rapid-annihilation WMAP ‘strip’ can appear at different values of  $\tan\beta$  and  $m_{1/2}$ , as seen in Fig. 6 [120, 121]. Rapid annihilation through the direct-channel  $H, A$  poles suppresses the relic density between the two parallel vertical WMAP strips at smaller values of  $m_{1/2}$ , and the relic density is suppressed in the right-most strip because the neutralino LSP has a significant higgsino component. A complete exploration of the parameter space of the NUHM, which has two additional parameters compared to the CMSSM, lies beyond the scope of this review.

The appearance of the  $(m_{1/2}, m_0)$  plane is also changed significantly if one assumes that the universality of soft super-symmetry-breaking masses in the CMSSM occurs not at the GUT scale, but at some lower renormalization scale [122, 123, 124], as occurs in some ‘mirage unification’ models [125, 126, 127]. In this case, the sparticle masses are generally closer together. As a consequence, the bulk, coannihilation, rapid-annihilation and focus-point regions approach each other and eventually merge as the mirage unification scale is reduced, as illustrated in Fig. 7, where they form an ‘atoll’. At smaller values of the mirage unification scale, the atoll contracts and eventually disappears, and there is no WMAP-compatible region within the displayed portion of the  $(m_{1/2}, m_0)$  plane. In such ‘GUTless’ models,  $\Omega_{LSP}h^2$  falls below the WMAP range (17) in larger regions of the  $(m_{1/2}, m_0)$  plane than in the conventional CMSSM with unification at the GUT scale.

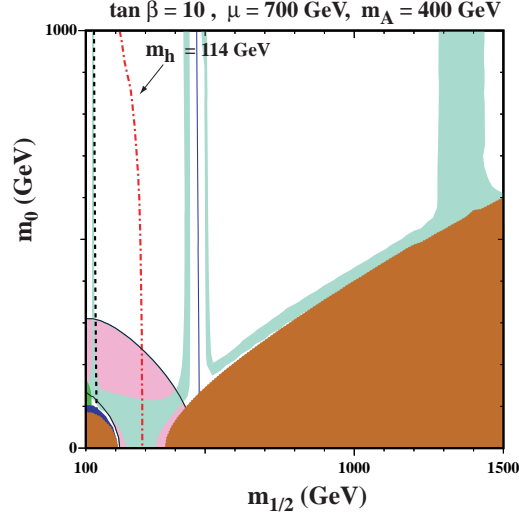


Figure 6: The  $(m_{1/2}, m_0)$  plane in the NUHM for  $\tan \beta = 10$ ,  $\mu = 700$  GeV and  $m_A = 400$  GeV [121]. The colours of the shadings and contours are the same as in Fig. 2.

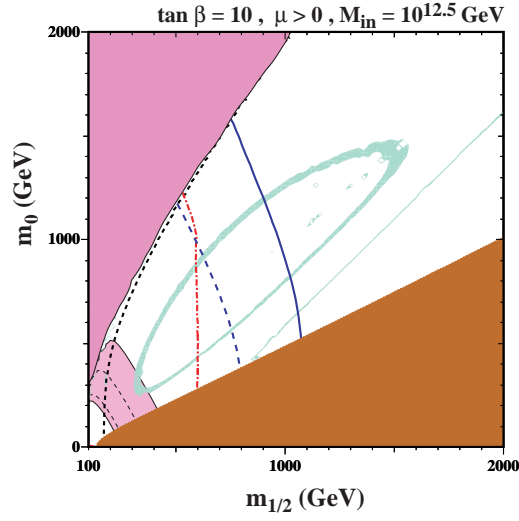


Figure 7: The  $(m_{1/2}, m_0)$  plane in a GUTless model with  $\tan \beta = 10$ ,  $\mu > 0$  and  $A_0 = 0$ , assuming universality at  $M_{in} = 10^{12.5}$  GeV [123]. The colours of the shadings and contours are the same as in Fig. 2.

## 8 Summary

As we have discussed above, there are many sound theoretical and phenomenological reasons to favour supersymmetric extensions of the Standard Model. In particular, supersymmetry predicts the existence of cold dark matter in a very natural way, and there are several plausible candidates for the lightest supersymmetric particle that would be present as a relic from the Big Bang. The most prominent candidate is the lightest neutralino, and we have described how its relic density may be calculated, and the regions of supersymmetric parameter space in which its density falls within the range favoured by astrophysics and cosmology. However, other candidates for the cold dark matter are also possible, such as the gravitino. In that case, the next-to-lightest supersymmetric particle would be metastable, and comparisons between the observed light-element abundances and those predicted by Big-Bang Nucleosynthesis calculations impose important constraints on the parameter space. We have given examples of neutralino and gravitino dark matter scenarios in the minimal supersymmetric extension of the Standard Model, under various different theoretical assumptions. It will be for collider and dark matter detection experiments to determine which, if any, of these options has been adopted by Nature.

## Acknowledgements

The work of K.A.O. was partially supported by DOE grant DE-FG02-94ER-40823.

## References

- [1] L. Maiani, in Proceedings, Gif-sur-Yvette Summer School On Particle Physics, 1979, 1-52.

- [2] Gerard 't Hooft and others (eds.), *Recent Developments in Gauge Theories, Proceedings of the Nato Advanced Study Institute, Cargese, France, August 26 - September 8, 1979*, Plenum press, New York, USA, 1980, Nato Advanced Study Institutes Series: Series B, Physics, 59.
- [3] Edward Witten, *Phys. Lett.* B105, 267, 1981.
- [4] H. Goldberg, *Phys. Rev. Lett.* 50, 1419, 1983.
- [5] John R. Ellis, J. S. Hagelin, Dimitri V. Nanopoulos, Keith A. Olive and M. Srednicki, *Nucl. Phys.* B238, 453, 1984.
- [6] John R. Ellis, S. Kelley and Dimitri V. Nanopoulos, *Phys. Lett.* B249, 441, 1990.
- [7] John R. Ellis, S. Kelley and Dimitri V. Nanopoulos, *Phys. Lett.* B260, 131, 1991.
- [8] Ugo Amaldi, Wim de Boer, and Hermann Furstenau. *Phys. Lett.*, B260, 447, 1991.
- [9] Paul Langacker and Ming-xing Luo, *Phys. Rev.* D44, 817, 1991.
- [10] C. Giunti, C. W. Kim and U. W. Lee, *Mod. Phys. Lett.* A6, 1745, 1991.
- [11] John R. Ellis, Giovanni Ridolfi and Fabio Zwirner, *Phys. Lett.* B257, 83, 1991.
- [12] John R. Ellis, Giovanni Ridolfi and Fabio Zwirner, *Phys. Lett.* B262, 477, 1991.
- [13] Y. Okada, Masahiro Yamaguchi and T. Yanagida, *Phys. Lett.* B262, 54, 1991.
- [14] Yasuhiro Okada, Masahiro Yamaguchi and Tsutomu Yanagida, *Prog. Theor. Phys.* 85, 1, 1991.

- [15] Howard E. Haber and Ralf Hempfling, *Phys. Rev. Lett.* 66, 1815, 1991.
- [16] LEP Electroweak Working Group, <http://lepewwg.web.cern.ch/LEPEWWG/>.
- [17] Tevatron Electroweak Working Group, <http://tevewwg.fnal.gov/>.
- [18] John R. Ellis and Douglas Ross, *Phys. Lett.* B506, 331, 2001, hep-ph/0012067.
- [19] G. W. Bennett *et al.*, *Phys. Rev.* D73, 072003, 2006, hep-ex/0602035.
- [20] M. Passera, W. J. Marciano and A. Sirlin, *Phys. Rev.* D78, 013009, 2008, arXiv:0804.1142 [hep-ph].
- [21] M. Davier, A. Hoecker, B. Malaescu, C. Z. Yuan and Z. Zhang, arXiv:0908.4300 [hep-ph].
- [22] P. Fayet and S. Ferrara, *Phys. Rept.* 32, 249, 1977.
- [23] Hans-Peter Nilles, *Phys. Rept.* 110, 1, 1984.
- [24] Pierre Fayet, *Phys. Lett.* B64, 159, 1976.
- [25] Pierre Fayet, *Phys. Lett.* B69, 489, 1977.
- [26] Pierre Fayet, *Phys. Lett.* B84, 416, 1979.
- [27] Howard E. Haber and Gordon L. Kane, *Phys. Rept.* 117, 75, 1985.
- [28] E. Cremmer *et al.*, *Nucl. Phys.* B147, 105, 1979.
- [29] E. Cremmer *et al.*, *Phys. Lett.* B79, 231, 1978.
- [30] Riccardo Barbieri, S. Ferrara, and Carlos A. Savoy, *Phys. Lett.* B119, 343, 1982.
- [31] Richard L. Arnowitt, Ali H. Chamseddine, and Pran Nath, *Phys. Rev. Lett.* 50, 232, 1983.

- [32] L. Girardello and Marcus T. Grisaru, *Nucl. Phys.* B194, 65, 1982.
- [33] Stephen P. Martin, hep-ph/9709356.
- [34] John R. Ellis, hep-ph/9812235.
- [35] Keith A. Olive, hep-ph/9911307.
- [36] Michael E. Peskin, arXiv:0801.1928 [hep-ph].
- [37] Glennys R. Farrar and Pierre Fayet, *Phys. Lett.* B76, 575, 1978.
- [38] J. Rich, D. Lloyd Owen and M. Spiro. *Phys. Rept.* 151, 239, 1987.
- [39] P. F. Smith, *Contemp. Phys.* 29, 159, 1988.
- [40] T. K. Hemmick *et al.*, *Phys. Rev.* D41, 2074, 1990.
- [41] Toby Falk, Keith A. Olive and Mark Srednicki, *Phys. Lett.* B339, 248, 1994, hep-ph/9409270.
- [42] LEP Collaborations, ALEPH, DELPHI, L3 and OPAL, LEP Electroweak Working Group, SLD Electroweak Group and SLD Heavy Flavor Group, hep-ex/0312023.
- [43] Mark Srednicki, Richard Watkins and Keith A. Olive, *Nucl. Phys.* B310, 693, 1988.
- [44] P. Hut, *Phys. Lett.* B69, 85, 1977.
- [45] Benjamin W. Lee and Steven Weinberg, *Phys. Rev. Lett.* 39, 165, 1977.
- [46] M. I. Vysotsky, A. D. Dolgov and Ya. B. Zeldovich, *JETP Lett.* 26, 188, 1977.
- [47] G. Steigman, Keith A. Olive and D. N. Schramm, *Phys. Rev. Lett.* 43, 239, 1979.

- [48] Keith A. Olive, David N. Schramm and Gary Steigman, *Nucl. Phys.* B180, 497, 1981.
- [49] Kim Griest and David Seckel, *Phys. Rev.* D43, 3191, 1991.
- [50] John R. Ellis, Are R. Raklev and Ola K. Oye, *JHEP* 10, 061, 2006, hep-ph/0607261.
- [51] J. L. Diaz-Cruz, John R. Ellis, Keith A. Olive and Yudi Santoso, *JHEP* 05, 003, 2007, hep-ph/0701229.
- [52] Yudi Santoso, arXiv:0709.3952 [hep-ph].
- [53] Kazunori Kohri and Yudi Santoso, arXiv:0811.1119 [hep-ph].
- [54] John R. Ellis, Keith A. Olive and Yudi Santoso, *JHEP* 10, 005, 2008, arXiv:0807.3736 [hep-ph].
- [55] Manuel Drees and Mihoko M. Nojiri, *Phys. Rev.* D47, 376, 1993, hep-ph/9207234.
- [56] Howard Baer and Michal Brhlik, *Phys. Rev.* D53, 597, 1996, hep-ph/9508321.
- [57] Howard Baer and Michal Brhlik, *Phys. Rev.* D57, 567, 1998, hep-ph/9706509.
- [58] Howard Baer *et al.*, *Phys. Rev.* D63, 015007, 2001, hep-ph/0005027.
- [59] A. B. Lahanas, Dimitri V. Nanopoulos and V. C. Spanos, *Mod. Phys. Lett.* A16, 1229, 2001, hep-ph/0009065.
- [60] John R. Ellis, Toby Falk, Keith A. Olive and Michael Schmitt, *Phys. Lett.* B388, 97, 1996, hep-ph/9607292.
- [61] John R. Ellis, Toby Falk, Keith A. Olive and Michael Schmitt, *Phys. Lett.* B413, 355, 1997, hep-ph/9705444.



- [62] John R. Ellis, Toby Falk, Gerardo Ganis, Keith A. Olive and Michael Schmitt, *Phys. Rev.*, D58, 095002, 1998, hep-ph/9801445.
- [63] Vernon D. Barger and Chung Kao, *Phys. Rev.* D57, 3131, 1998, hep-ph/9704403.
- [64] John R. Ellis, Toby Falk, Gerardo Ganis and Keith A. Olive, *Phys. Rev.* D62, 075010, 2000, hep-ph/0004169.
- [65] Vernon D. Barger and Chung Kao, *Phys. Lett.* B518, 117, 2001, hep-ph/0106189.
- [66] Leszek Roszkowski, Roberto Ruiz de Austri and Takeshi Nihei, *JHEP* 08, 024, 2001, hep-ph/0106334.
- [67] A. B. Lahanas and V. C. Spanos, *Eur. Phys. J.* C23, 185, 2002, hep-ph/0106345.
- [68] A. Djouadi, Manuel Drees and J. L. Kneur, *JHEP* 08, 055, 2001, hep-ph/0107316.
- [69] Utpal Chattopadhyay, Achille Corsetti and Pran Nath, *Phys. Rev.* D66, 035003, 2002, hep-ph/0201001.
- [70] John R. Ellis, Keith A. Olive and Yudi Santoso, *New J. Phys.* 4, 32, 2002, hep-ph/0202110.
- [71] Howard Baer *et al.*, *JHEP* 07, 050, 2002, hep-ph/0205325.
- [72] Richard L. Arnowitt and Bhaskar Dutta, hep-ph/0211417.
- [73] John R. Ellis, Toby Falk, Gerardo Ganis, Keith A. Olive and Mark Srednicki, *Phys. Lett.* B510, 236, 2001, hep-ph/0102098.
- [74] John R. Ellis, Keith A. Olive, Yudi Santoso and Vassilis C. Spanos, *Phys. Lett.* B565, 176, 2003, hep-ph/0303043.

- [75] Howard Baer and Csaba Balazs, *JCAP* 0305, 006, 2003, hep-ph/0303114.
- [76] A. B. Lahanas and Dimitri V. Nanopoulos, *Phys. Lett.* B568, 55, 2003, hep-ph/0303130.
- [77] Utpal Chattopadhyay, Achille Corsetti, and Pran Nath, *Phys. Rev.* D66, 035003, 2002, hep-ph/0201001.
- [78] Carlos Munoz, *Int. J. Mod. Phys.* A19, 3093, 2004, hep-ph/0309346.
- [79] Luis E. Ibanez and Graham G. Ross, *Phys. Lett.* B110, 215, 1982.
- [80] Luis E. Ibanez, *Phys. Lett.* B118, 73, 1982.
- [81] John R. Ellis, Dimitri V. Nanopoulos and K. Tamvakis, *Phys. Lett.* B121, 123, 1983.
- [82] John R. Ellis, J. S. Hagelin, Dimitri V. Nanopoulos and K. Tamvakis, *Phys. Lett.* B125, 275, 1983.
- [83] Luis Alvarez-Gaume, J. Polchinski, and Mark B. Wise, *Nucl. Phys.*, B221, 495, 1983.
- [84] Joint LEP 2 Supersymmetry Working Group,  
[http://lepsusy.web.cern.ch/lepsusy/www/inos\\_moriond01/charginos\\_pub.html](http://lepsusy.web.cern.ch/lepsusy/www/inos_moriond01/charginos_pub.html).
- [85] Joint LEP 2 Supersymmetry Working Group,  
[http://lepsusy.web.cern.ch/lepsusy/www/sleptons\\_summer02/slep\\_2002.html](http://lepsusy.web.cern.ch/lepsusy/www/sleptons_summer02/slep_2002.html).
- [86] R. Barate *et al.*, *Phys. Lett.* B565, 61, 2003, hep-ex/0306033.

- [87] LEP Higgs Working Group for Higgs boson searches, LHWG-NOTE-2004-01, ALEPH-2004-008, DELPHI-2004-042, L3-NOTE-2820, OPAL-TN-744, <http://lephiggs.web.cern.ch/LEPHIGGS/papers/August2004.MSSM/index.html>.
- [88] S. Heinemeyer, W. Hollik and G. Weiglein, *Comput. Phys. Commun.* **124**, 76, 2000, hep-ph/9812320.
- [89] S. Heinemeyer, W. Hollik and G. Weiglein, *Eur. Phys. J. C* **9**, 343, 1999, hep-ph/9812472.
- [90] E. Barberio *et al.*, hep-ex/0603003.
- [91] G. Degrandi, P. Gambino and G. F. Giudice, *JHEP* **12**, 009, 2000, hep-ph/0009337.
- [92] J. Dunkley *et al.* [WMAP Collaboration], *Astrophys. J. Suppl.* **180**, 306 (2009) [arXiv:0803.0586 [astro-ph]].
- [93] Jonathan L. Feng, Konstantin T. Matchev and Takeo Moroi, *Phys. Rev. D* **61**, 075005, 2000, hep-ph/9909334.
- [94] John R. Ellis, Keith A. Olive, Yudi Santoso and Vassilis C. Spanos, *Phys. Rev. D* **69**, 095004, 2004, hep-ph/0310356.
- [95] John R. Ellis, S. Heinemeyer, K. A. Olive, A. M. Weber and G. Weiglein, *JHEP* **08**, 083, 2007, arXiv:0706.0652 [hep-ph].
- [96] O. Buchmueller *et al.*, *Phys. Lett. B* **657**, 87, 2007, arXiv:0707.3447 [hep-ph].
- [97] O. Buchmueller *et al.*, *JHEP* **09**, 117, 2008, arXiv:0808.4128 [hep-ph].
- [98] *ATLAS Technical Design Report, vol. 2: Detector and Physics Performance*, CERN-LHCC-99-15.

- [99] G. L. Bayatian *et al.*, *CMS Technical Design Report, vol. 2: Physics Performance*, *J. Phys.* G34, 995, 2007.
- [100] Richard H. Cyburt, John R. Ellis, Brian D. Fields, Keith A. Olive and Vassilis C. Spanos, *JCAP* 0611, 014, 2006, astro-ph/0608562.
- [101] Richard H. Cyburt, Brian D. Fields and Keith A. Olive, arXiv:0808.2818 [astro-ph].
- [102] M. Pospelov, *Phys. Rev. Lett.* **98**, 231301 (2007) [arXiv:hep-ph/0605215].
- [103] K. Hamaguchi, T. Hatsuda, M. Kamimura, Y. Kino and T. T. Yanagida, *Phys. Lett.* B650, 268, 2007, hep-ph/0702274.
- [104] Chris Bird, Kristen Koopmans and Maxim Pospelov, *Phys. Rev.* D78, 083010, 2008, hep-ph/0703096.
- [105] Karsten Jedamzik, *Phys. Rev.* D70, 063524, 2004, astro-ph/0402344.
- [106] Karsten Jedamzik, *Phys. Rev.* D70, 083510, 2004, astro-ph/0405583.
- [107] A. Brignole, Luis E. Ibanez and C. Munoz, hep-ph/9707209.
- [108] John R. Ellis, Keith A. Olive, Yudi Santoso and Vassilis C. Spanos, *Phys. Lett.* B573, 162, 2003, hep-ph/0305212.
- [109] John R. Ellis, Keith A. Olive, Yudi Santoso and Vassilis C. Spanos, *Phys. Rev.* D70, 055005, 2004, hep-ph/0405110.
- [110] J. Polonyi, Hungary Central Inst Res - KFKI-77-93.
- [111] Jonathan L. Feng, Arvind Rajaraman and Fumihiro Takayama, *Phys. Rev. Lett.* 91, 011302, 2003, hep-ph/0302215.
- [112] John R. Ellis, Keith A. Olive, Yudi Santoso and Vassilis C. Spanos, *Phys. Lett.* B588, 7, 2004, hep-ph/0312262.

- [113] Jonathan L. Feng, Shufang Su and Fumihiro Takayama, *Phys. Rev. D* **70**, 075019, 2004, hep-ph/0404231.
- [114] Richard H. Cyburt, John R. Ellis, Brian D. Fields and Keith A. Olive, *Phys. Rev. D* **67**, 103521, 2003, astro-ph/0211258.
- [115] Jonathan L. Feng, Shu-fang Su and Fumihiro Takayama, *Phys. Rev. D* **70**, 063514, 2004, hep-ph/0404198.
- [116] John R. Ellis, Keith A. Olive and Elisabeth Vangioni, *Phys. Lett. B* **619**, 30, 2005, astro-ph/0503023.
- [117] Kazunori Kohri, Takeo Moroi and Akira Yotsuyanagi, *Phys. Rev. D* **73**, 123511, 2006, hep-ph/0507245.
- [118] David G. Cerdeno, Ki-Young Choi, Karsten Jedamzik, Leszek Roszkowski and Roberto Ruiz de Austri, *JCAP* **0606**, 005, 2006, hep-ph/0509275.
- [119] Frank Daniel Steffen, *JCAP* **0609**, 001, 2006, hep-ph/0605306.
- [120] John R. Ellis, Keith A. Olive and Yudi Santoso, *Phys. Lett. B* **539**, 107, 2002, hep-ph/0204192.
- [121] John R. Ellis, Toby Falk, Keith A. Olive and Yudi Santoso, *Nucl. Phys. B* **652**, 259, 2003, hep-ph/0210205.
- [122] John R. Ellis, Keith A. Olive and Pearl Sandick, *Phys. Lett. B* **642**, 389, 2006, hep-ph/0607002.
- [123] John R. Ellis, Keith A. Olive and Pearl Sandick, *JHEP* **06**, 079, 2007, arXiv:0704.3446 [hep-ph].
- [124] John R. Ellis, Keith A. Olive and Pearl Sandick, *JHEP* **08**, 013, 2008, arXiv:0801.1651 [hep-ph].

- [125] Kiwoon Choi, Adam Falkowski, Hans-Peter Nilles and Marek Olechowski, *Nucl. Phys.* B718, 113, 2005, hep-th/0503216.
- [126] Kiwoon Choi, Kwang Sik Jeong and Ken-ichi Okumura, *JHEP* 09, 039, 2005, hep-ph/0504037.
- [127] Adam Falkowski, Oleg Lebedev and Yann Mambrini, *JHEP* 11, 034, 2005, hep-ph/0507110.